

O⁺ observations in the cusp: Implications for dayside magnetic field topology

S. A. Fuselier, S. M. Petrinec, K. J. Trattner, and W. K. Peterson
Lockheed Martin Advanced Technology Center

Abstract

Under conditions of sustained northward IMF, magnetospheric magnetic field lines on the dayside may undergo multiple reconnection, producing closed flux tubes filled with solar wind plasma. Ionospheric O⁺ beams with energies of ~ 1 keV/e that are propagating parallel to the magnetic field in the northern cusp region are potential evidence for this multiple reconnection process. Using observations from the Polar spacecraft, we present evidence of parallel propagating O⁺ in the northern cusp. A statistical study of these events indicates that they are very rare in the Polar data. Therefore, the occurrence frequency of multiple reconnection on the dayside under northward IMF conditions appears to be insufficient to account for the nearly continuous population of solar wind plasma on closed field lines in the magnetosphere.

Introduction

Composition measurements in the Earth's plasma sheet clearly indicate that solar wind plasma has access to closed magnetic field lines. *Lennartsson* [1992] showed that the plasma sheet was most "solar wind-like" (i.e., the He²⁺/H⁺ density ratio was most similar to that in the solar wind) during periods of low geomagnetic activity and sustained northward IMF. During periods of high geomagnetic activity and sustained southward IMF, *Lennartsson* [1992] found a

higher ionospheric ion contribution to the plasma sheet, but found a persistent solar wind contribution as well.

These plasma sheet observations indicate that solar wind plasma must cross the magnetopause and gain access to the magnetosphere independent of the IMF orientation. For southward IMF, there is considerable evidence that magnetic reconnection occurs at the magnetopause and that solar wind plasma crosses the open boundary and enters the low latitude boundary (LLBL) [e.g., *Fuselier, 1995; Sonnerup et al., 1995*]. For northward IMF, there is also evidence that reconnection occurs and plasma is transferred across an open magnetopause. For example, *Fuselier et al. [1997]* reported observations consistent with an open dayside magnetopause more than 90% of the time during periods of northward IMF and high solar wind dynamic pressure. Thus, magnetic reconnection may be responsible for plasma transfer across the magnetopause independent of the IMF orientation.

Although reconnection appears to be a strong candidate for plasma transfer across the magnetopause, there is an important difficulty with this process. While solar wind plasma crosses the magnetopause, it is still on open field lines in regions such as the LLBL, cusp, or the mantle. Therefore, solar wind plasma access to closed field lines in the plasma sheet requires additional transfer processes (and/or additional reconnection) as well as transport from the dayside to the nightside. Additional transfer processes may include diffusion and non-linear growth of wave instabilities such as the Kelvin-Helmholz instability at the flank magnetopause (see the recent review of plasma entry processes by *Hultqvist et al. [1999]*).

Multiple reconnection is also a process which may produce closed flux tubes of solar wind plasma in the magnetosphere, particularly for northward IMF conditions. Figure 1 illustrates one possible multiple reconnection sequence. In the upper right of Figure 1,

magnetosheath field lines are labeled 1 through 4. The draped magnetosheath field line, (1), reconnects with a field line in the high latitude magnetosphere poleward of the southern cusp (2). The newly reconnected field line drapes against the dayside magnetosphere and the location where the field line crosses the magnetopause moves from southern high latitudes, through the equatorial region, to northern high latitudes (3 and 4). At northern high latitudes the reconnected field line (4) may reconnect again, forming a closed field line of magnetosheath plasma that is contained entirely within the magnetosphere. Magnetospheric convection causes this field line to convect to the nightside where it ultimately becomes part of the plasma sheet (not shown).

Several authors have suggested multiple reconnection processes similar to the one illustrated in Figure 1 [e.g., *Dungey*, 1963]. Variations on this process include near-simultaneous reconnection poleward of both cusps [*Song and Russell*, 1992] and multiple patchy reconnection producing several field line topologies on the dayside [*Nishida*, 1989]. Multiple reconnection similar to that in Figure 1 is also seen in global MHD simulations [e.g., *Wu*, 1983; *Berchem et al.*, 1995; *Russell et al.*, 1998]. Finally, although Figure 1 illustrates this reconnection process for purely northward IMF, potential reconnection sites (i.e., sites where the magnetosheath and magnetospheric field lines are antiparallel) can be found at the high latitude magnetopause poleward of both cusps for northward IMF orientations that have a B_y component [e.g., *Crooker*, 1979; *Song and Russell*, 1992].

There is considerable evidence at the magnetopause for high latitude reconnection poleward of the cusp (i.e., field lines 1 and 2 in Figure 1) [e.g., *Gosling et al.*, 1991; *Kessel et al.*, 1996]. Observations in the cusp consistent with this single reconnection site include sunward convection of cusp field lines [e.g., *Maeszawa*, 1976] which produce an energy-latitude dispersion of the entering magnetosheath ions. Highest energy magnetosheath ions are observed at the

highest cusp latitudes and successively lower energies are observed at lower latitudes [e.g., *Woch and Lundin*, 1992]. The cusp ion distributions observed during high latitude reconnection can be used to find the location of the reconnection site. Using cusp observations from the Polar spacecraft and a model field, the reconnection site at high latitudes poleward of the cusp was recently confirmed [*Fuselier et al.*, 2000].

In the equatorial, subsolar region, uni-directional streaming ions and electrons in a thin boundary layer just sunward of the magnetopause are also evidence for high latitude reconnection [*Fuselier et al.*, 1995]. In Figure 1, the electrons and ions stream parallel to the magnetic field along field lines 2, 3, and 4 because the first reconnection site is at southern high latitudes. Additional evidence for high latitude reconnection is also shown in Figure 1. In a study of subsolar magnetopause crossings under northward IMF and high solar wind dynamic pressure conditions, ionospheric O⁺ beams such as the one in Figure 1 were observed in the LLBL (earthward of the magnetopause) in 50% of the cases. The origin of these beams is illustrated in Figure 1. Ionospheric outflow in the cusp region is essentially continuous [e.g., *Yau et al.*, 1985]. Under southward IMF conditions, these ionospheric ions propagate tailward along with the antisunward convecting lobe field lines. However, for northward IMF, the convection is sunward and ionospheric H⁺, He⁺, and O⁺ follow the reconnected lobe field lines into the dayside LLBL. For the observations in the subsolar region, there is an important consistency check for this process. The direction of propagation of ~1 keV/e O⁺ beams in the LLBL should be the same as the direction of propagation of the energetic electrons observed on reconnected field lines sunward of the magnetopause (e.g., field line 2 in Figure 1). In 5 of 5 cases of persistent northward IMF investigated by *Fuselier et al.* [1997], the direction of propagation of

the electrons and the ionospheric ions was the same and therefore consistent with high latitude reconnection.

The observation of unidirectional O^+ beams in the subsolar LLBL during periods of persistent northward IMF is evidence that the magnetic field may remain open long after the initial reconnection. However, if the field line reconnects again in the opposite cusp (the northern cusp in Figure 1), then this second reconnection allows O^+ from one hemisphere to precipitate in the opposite high latitude cusp region. This would also produce bi-directional streaming O^+ in the LLBL. Bi-directional streaming O^+ was not seen in the subsolar LLBL in the limited number of events (10 events total) with persistent northward IMF investigated by *Fuselier et al.* [1997]. These limited results notwithstanding, parallel (antiparallel) propagating O^+ beams with energies ~ 1 keV/e in the northern (southern) cusp during periods of sustained northward IMF is potential evidence for multiple reconnection.

In this paper, we present an event from the Polar spacecraft which exhibits evidence of parallel propagating (toward the ionosphere) ~ 1 keV/e O^+ in the northern cusp during persistent northward IMF. The solar wind ion precipitation in the cusp during this event is consistent with high latitude reconnection poleward of the northern cusp. Thus, the combined solar wind and ionospheric ion observations are consistent with reconnection in both cusps and the formation of closed flux tubes of solar wind plasma in the dayside magnetosphere. Statistics presented after the discussion of this event indicate that this type of event is rarely observed in the Polar data.

Instrumentation

Observations in this paper are from the Toroidal Imaging Mass Angle Spectrograph (TIMAS) instrument on the Polar spacecraft [Shelley *et al.*, 1995]. Polar is in a 90° inclination orbit which precesses through 24 hours of local time in one year. Thus, for two periods each year (in the spring and fall), the orbit cuts through the dayside cusp. During these periods, the TIMAS instrument makes mass resolved, full three-dimensional velocity space measurements of the major solar wind (H^+ and He^{2+}) and ionospheric (H^+ , He^+ , and O^+) ions in 1 to 2 spacecraft spins (6-12 s). Pitch angle and ion propagation direction information were obtained by combining these TIMAS observations with measurements of the magnetic field from the Magnetic Field Investigation (MFI) [Russell *et al.*, 1995]. In addition to these high resolution measurements, the TIMAS instrument compiles a mass spectrum (64 mass steps covering the mass per charge range from 1 to >32) at 8 energies and 6 angles. The time resolution of these spectra depends on the instrument mode, but for the data discussed here, a mass spectrum was obtained in 32 spins (~3 min). These mass spectra are critical for confirmation of the presence of O^+ because H^+ fluxes contaminate higher mass fluxes in the TIMAS instrument. This contamination depends on the H^+ flux level and is typically significant for high fluxes in the cusp at energies <1 keV/e.

Cusp observations in this paper are related to IMF conditions observed on the Wind spacecraft [Lepping *et al.*, 1995]. This upstream monitor is typically located many 10's of R_E from the Earth and IMF observations in this paper are always convected to the cusp using the position of the Wind spacecraft and the observed solar wind flow velocity.

Observations on 11 October 1997

Figure 2 shows an overview of the TIMAS observations on 11 October 1997. The three panels contain the omnidirectional flux (24 s time resolution) of H^+ , He^{2+} , and O^+ in an energy-time format. During this one hour interval, the spacecraft moved from 74° to 64.5° magnetic latitude and from 6.85 to $5.9 R_E$ radial distance along a trajectory nearly at noon magnetic local time. Throughout the interval in Figure 2, the IMF (as measured by the Wind spacecraft) was northward. At approximately 1620 UT, the H^+ and He^{2+} fluxes above about 1 keV/e increased dramatically, indicating the presence of solar wind ions and entry into the cusp. Starting at about 1630 UT, the high fluxes of solar wind H^+ and He^{2+} are seen more continuously. From this time until 1712 UT, the energy of maximum solar wind ion flux steadily decreases from above 1 keV/e to 0.1 keV/e. As discussed in the introduction, this energy-latitude dispersion is consistent with reconnection poleward of the northern cusp.

The ion velocity space distributions obtained near the poleward edge of the cusp (1620-1640 UT) also show features consistent with high latitude reconnection poleward of the cusp. Figure 3 shows one of the H^+ distributions seen near this edge of the cusp. The left hand side of the figure shows the spacecraft location (solid dot) in the Tsyganenko 1996 model magnetic field. According to the model, the spacecraft is located on a lobe field line. This field line crosses the equator in the distant tail and follows the magnetopause at high latitudes between $X_{GSM} = -2 R_E$ to $X = 2 R_E$ in Figure 3 before turning southward and terminating at high northern latitudes. A closed dayside magnetospheric field line which crosses the equator at the noon meridian is shown for comparison to this lobe field line.

The right hand side of Figure 3 is slice through the 3 dimensional H^+ distribution observed on the lobe field line. Contours of constant phase space density with two contours per decade are shown. The origin is zero velocity in the spacecraft frame and velocities parallel to

the magnetic field are along the positive y-axis. Dots in the contour plot show the location of energy-angle measurements that went into constructing the phase space contours. Below this contour plot is a cut along the magnetic field, showing the phase space density of zero pitch angle particles. Solid lines in this cut are the measured phase space densities and dashed lines are one-sigma levels.

For zero pitch angles and phase space densities above one sigma, the H⁺ distribution in Figure 3 consists of two populations. The first population is propagating parallel to the magnetic field (toward the ionosphere, or earthward) with a velocity of approximately 300 km/s. The second population is propagating antiparallel to the magnetic field (away from the ionosphere, or mirrored at low altitudes) with a velocity of approximately -600 km/s. Both populations have sharp velocity space cutoffs labeled V_e (earthward) and V_m (mirrored) in the cut in Figure 3.

Here, we interpret the parallel propagating population as the entering magnetosheath H⁺ and the antiparallel propagating population as the magnetosheath population that entered the magnetosphere, mirrored at low altitudes, and returned to the spacecraft. With this interpretation, the cutoff velocities V_e and V_m in Figure 3 are evidence of the finite extent of the reconnection region and are used to determine the distance along the magnetic field from the spacecraft to the reconnection site. As discussed in detail by *Onsager et al.* [1990] and *Fuselier et al.* [2000], the distance from the spacecraft to the reconnection site, X_r, is related to the distance from the spacecraft to the mirror point, X_m, by:

$$\frac{X_r}{X_m} = \frac{2V_e}{(V_m - V_e)} \quad (1)$$

where V_e and V_m are the absolute values of the cutoff velocities in Figure 3. Equation 1 is obtained by equating the travel time for ions directly from the reconnection site (at the earthward directed cutoff velocity) with the travel time for ions that originated at the reconnection site, mirrored at low altitudes, and returned to the spacecraft (at the mirrored cutoff velocity). The spacecraft was located approximately $X_m=6 R_E$ from the mirror point (see Figure 3). Using the measured V_e and V_m in Figure 3, X_m , and Equation 1, the distance to the reconnection site, $X_r = 4.4 \pm 0.8 R_E$. This reconnection site location is shown by the open circle on the field line in the left hand side of Figure 3. The uncertainty in the location of the reconnection site (shown by the two short lines on either side of the open circle) is directly related to the uncertainty in the measurement of V_e and V_m in Figure 3 (see *Fuselier et al.* [2000]).

The reconnection site is very close to where the field line parallels the magnetopause and it indicates that the lobe field line poleward of the cusp was undergoing reconnection with the draped magnetosheath field line (not shown). Subsequent ion distributions observed in the interval from 1640 to 1712 UT (also not shown here) exhibit a gradual decrease in the cutoff velocity of the parallel and antiparallel propagating ion populations seen in Figure 3. The gradual decrease in the cutoff velocities manifests itself as a gradual decrease in the energy of maximum H^+ flux in Figure 2. The gradual decrease in the cutoff velocities is consistent with a relatively stable reconnection site at high latitudes poleward of the cusp and spacecraft motion to lower latitudes during the cusp interval.

The bottom panel of Figure 2 shows that ionospheric O^+ is relatively weak and approximately monoenergetic in the cusp from 1630 to 1704 UT. Like the solar wind ion energy, the energy of maximum flux for ionospheric O^+ decreases with decreasing latitude. At 1704 UT, the O^+ flux increases dramatically and remains high up to and through the equatorial

edge of the cusp (i.e., after 1712 UT). Some of the flux seen in the bottom panel is not O^+ , rather it is H^+ flux which contaminates the O^+ mass channels when the H^+ flux is high. This contamination makes it difficult to distinguish the propagation direction of the O^+ population in the cusp using the high time resolution O^+ observations.

In addition to high resolution ion distributions, the TIMAS instrument accumulates mass spectra over 64 mass steps, 6 angle sectors, and 8 energies during a 32 spin (~ 3 min) interval. Four of the angle sectors have centers in the spin plane and the other two angle sectors are parallel and antiparallel to the spacecraft spin axis. Thus, in 32 spins (~ 3 min), mass spectra are obtained at 8 energies and in $90^\circ \times 90^\circ$ angle bins which cover the unit sphere. The energy range of these spectra depends on the TIMAS operations mode. For the event in Figure 2, the 8 energies span (but are not contiguous over) the full TIMAS energy range from 0.016 keV/e to 40 keV/e. For the study here, we use the two measured energies closest to 1 keV/e.

Figure 4 shows a mass spectrum at 1.72 keV/e for ion propagation parallel (open circles) and antiparallel (filled circles) to the magnetic field at 1651-54 UT. The count rate is normalized by the peak count rate and major ion species are labeled at their nominal mass channel positions (the mass channel position of an ion species is a function of energy in the TIMAS instrument). During this interval, there is clearly H^+ and He^{2+} propagating both parallel and antiparallel to the magnetic field. The He^{2+}/H^+ ratio is about 3%, consistent with a dominant solar wind H^+ component both parallel and antiparallel to the magnetic field. In contrast to the solar wind ions, the O^+ in Figure 4 is propagating only antiparallel to the magnetic field (i.e., away from the ionosphere). Figure 5 shows the similar mass spectra at two energies that were measured near the equatorial edge of the cusp (1707-1710 UT) during the period when the O^+ flux increased dramatically (see Figure 2). In Figure 5, there are H^+ , He^{2+} , and O^+ populations propagating

both parallel and antiparallel to the magnetic field. Relative to H^+ , the parallel and antiparallel O^+ fluxes are nearly equal. The absolute H^+ flux parallel to the magnetic field was nearly equal to that antiparallel to the magnetic field for both energies in Figure 5. Thus, there are equal fluxes of O^+ flux propagating toward and away from the northern ionosphere at these energies.

Mass spectra similar to those in Figures 4 and 5 are used to verify the presence of O^+ over the entire cusp interval in Figure 2. The average counts centered on the O^+ peak (mass steps 32-36 for 0.68 keV/e and mass steps 36-42 for 1.7 keV/e in Figure 5) is compared to the average counts between the He^+ and O^+ peaks (mass steps 29-31 for 0.68 keV/e and mass steps 33-35 for 1.7 keV/e in Figure 5). The “background” measure is actually in the mass range of O^{2+} , but there is very little O^{2+} present in the cusp compared to O^+ .

Figure 6 shows the relative count rate of antiparallel propagating O^+ at 0.68 and 1.72 keV/e for the one hour interval in Figure 2. Figure 7 shows the same thing for parallel propagating O^+ . In Figure 6, the antiparallel propagating O^+ is not above background until after 1645 UT. Thus, the weak O^+ flux seen in Figure 2 from 1630 to 1645 UT is largely H^+ flux that is contaminating the O^+ mass channels. However starting after 1645 UT in Figure 6, the antiparallel propagating O^+ at 1.72 keV/e is above background and later the flux at 0.68 keV/e is above background. Thus, O^+ outflow from the ionosphere has a similar energy-latitude dispersion as the H^+ and He^{2+} from the solar wind. The similarity between the dispersion of the ionospheric and solar wind fluxes is relatively easy to interpret. For ionospheric O^+ outflow confined to a relatively narrow range of latitudes, the sunward convection of the reconnected field lines will cause the same energy latitude dispersion in this finite source as the dispersion for the solar wind population entering along reconnected field lines.

In Figure 7, the parallel propagating O^+ remains below the background level until after the O^+ flux increase (starting at 1704 UT in Figure 2). Only the last two mass spectra nearest the equatorial edge of the cusp show evidence of an O^+ population that is parallel to the magnetic field (i.e., propagating toward the ionosphere). Under the interpretation that reconnected field lines in the cusp are convecting sunward, the field lines at the equatorial edge of the cusp have been reconnected for the longest period of time. If the O^+ is from the southern high latitude ionosphere, then it is no coincidence that earthward propagating O^+ is observed on these field lines. O^+ with an energy of ~ 1 keV/e ($V_{\parallel} \sim 100$ km/s) is traveling at a speed of approximately $1 R_E/\text{min}$ and will take 20-30 min to propagate from the high latitude southern ionosphere to the Polar spacecraft location in the high latitude northern ionosphere. This observation of earthward directed O^+ near the equatorial edge of the northern cusp is therefore consistent with the multiple reconnection process illustrated in Figure 1.

Statistical Study

As discussed in the introduction, the occurrence frequency of multiple reconnection has important implications on the access of solar wind plasma to closed magnetic flux tubes in the magnetosphere. How often parallel propagating O^+ is observed in the northern cusp from the Polar spacecraft is a measure of this occurrence frequency. TIMAS observations in the cusp from fall 1996 through fall 1997 were used in a statistical study of parallel propagating O^+ in the cusp. Cusp events were chosen when the IMF remained northward at least 20 min prior to the start of the interval and remained northward during the interval. In some cases, the IMF began

northward but turned southward during the cusp interval. For these events, only the cusp interval up to the southward turning was used.

Over the 1.5 year period, 60 cusp intervals satisfied the IMF orientation criterion. During these 60 cusp intervals, 1278 mass spectra were obtained. For each mass spectrum, the O⁺ countrates at 0.68 and 1.72 keV/e (i.e., the two measured energies nearest 1 keV/e) relative to the background countrates were determined for parallel and antiparallel propagating directions using the same method described for Figures 6 and 7. Table 1 contains the statistical results of the search for O⁺ fluxes above background in these two propagation directions.

In Table 1, antiparallel propagating O⁺ (i.e., outflow from the ionosphere) was observed at least 50% of the time. This result does not imply that the other 50% of the time there was no ion outflow. Unlike previous studies of ion outflow (e.g., *Yau et al.* [1985]) used a very broad energy range from 10 eV/e to over 10 keV/e. In contrast, this study considers outflow over a very narrow energy range centered on 1 keV/e. Outflow above 1 keV/e was less common than below this energy (35% of the time for 1.7 keV/e compared to 48% of the time for 0.68 keV/e) because ionospheric O⁺ outflow is typically energized to <1 keV/e [*Yau et al.*, 1985]. Spectra with parallel propagating O⁺ (i.e., O⁺ possibly from the southern high latitude ionosphere) were very rare in the cusp.

As discussed in the previous section, the relatively low velocity of O⁺ beams originating in the southern ionosphere suggests that these beams will be observed in the northern hemisphere only on multiply reconnected field lines near the equatorial edge of the cusp. Thus, the fact that there are few spectra in the northern cusp with parallel propagating O⁺ does not necessarily imply that multiple reconnection and the formation of closed cusp field lines is an uncommon

process. After all, only 2 of the 15 spectra in Figure 7 at 0.68 keV/e or at 1.72 keV/e show evidence of parallel propagating O⁺.

Table 2 shows that even when considered on an event by event basis, parallel propagating O⁺ rarely occurs in the cusp. Of the 60 events, only 6 (10%) of the events had at least one spectrum with parallel propagating 0.68 or 1.72 keV/e O⁺. In all 6 of these events, parallel propagating O⁺ was observed in only a small part of the cusp interval near the equatorial edge. Thus, although there are events similar to the one discussed in Figures 2 through 7, these events are rare.

Discussion and Conclusions

In this paper, we discussed an event which is consistent with multiple reconnection and formation of closed field lines in the dayside magnetosphere. There are several features of this event which can be interpreted in this fashion.

- 1) The event occurs during a period of prolonged northward IMF, which is conducive to high latitude reconnection [e.g., *Dungey*, 1963].
- 2) Energy-latitude dispersion and details of the solar wind velocity space distributions indicate that high latitude reconnection was occurring poleward of the northern cusp (Figures 2 and 3).
- 3) Antiparallel propagating O⁺ (ion outflow from the northern ionosphere) also exhibits energy-latitude dispersion consistent with sunward convection of the reconnected magnetic field lines (Figure 6).

4.) Parallel propagating O^+ (possible ion outflow from the southern hemisphere) is observed only on those field lines that have been reconnected the longest. This observation is consistent with the relatively slow convection speed of the O^+ along the magnetic field and the significant distance from the southern ionosphere along a field that threads the LLBL and connects to the northern ionosphere.

The results of a search for more events like the one in Figures 2 through 7 indicate that this type of event is rare. The statistics in Tables 1 and 2 are consistent with the paucity of reports of parallel propagating O^+ in the cusp. In fact, we can find only one reference in the literature to parallel propagating O^+ in the cusp [*Peterson et al.*, 1985]. *Dempsey et al.* [1998] report an event with parallel propagating O^+ and solar wind ions on the same field line. However, the parallel propagating O^+ was observed at nearly 1700 magnetic local time, well outside the local time of the cusp [e.g., *Newell and Meng*, 1992].

One possible explanation for the rare occurrence of parallel propagating ~ 1 keV/e O^+ in the northern cusp is that the beams originating in the southern hemisphere are scattered by some unknown mechanism prior to arriving in the northern hemisphere. This explanation is not consistent with observations in the subsolar region. *Fuselier et al.* [1997] reported ~ 1 keV/e O^+ beams for 50% of the subsolar magnetopause crossings with persistent northward IMF. This occurrence frequency of ~ 1 keV/e O^+ in the LLBL is the same as the occurrence frequency of O^+ outflow at ~ 1 keV/e from northern high latitudes (Table 1) when considered on a spectrum by spectrum basis. When considered on an event by event basis, ion outflow at ~ 1 keV/e from northern high latitudes occurred 80% of the time (Table 2). Thus, it appears that O^+ beams

leaving the high latitude ionosphere have essentially unrestricted access to the dayside magnetopause region. This region is located halfway between the two high latitude ionospheres.

Similarly, the high occurrence frequency of O⁺ beams in the LLBL from *Fuselier et al.* 1997] indicates that the reconnected field remains on the dayside for a long period of time. Certainly long enough for the ionospheric ions to complete half of the distance to the opposite hemisphere.

The low occurrence frequency of parallel propagating O⁺ in the cusp in Table 1 is consistent with the lack of bidirectional streaming O⁺ in the LLBL for periods of sustained northward IMF [*Fuselier et al.*, 1997]. The data set of LLBL intervals was much smaller than the one used here (10 LLBL events compared to 60 cusp events) and therefore it is not surprising that no bidirectional streaming O⁺ was observed in the LLBL.

Another possible explanation for the results in Tables 1 and 2 is that the ion outflow from one hemisphere may be less than from the other. However, this would require a systematic asymmetry in the outflow from the northern and southern hemispheres. If the average outflow was the same, then conditions for observing parallel propagating O⁺ in the northern hemisphere should be favorable at least 50% of the time. Also, if such asymmetries were important, then there could be favorable seasonal periods or dipole tilt orientations for observing parallel propagating O⁺ in the northern hemisphere. For example, a dipole tilt away from the sun could favor initial reconnection in the southern cusp so that when the field line reconnects a second time in the northern cusp, it already contains O⁺ beams from the southern ionosphere (as illustrated in Figure 1). Although not shown here, the events in Table 2 with parallel propagating O⁺ exhibit no dipole tilt or seasonal preferences.

In addition to the southern high latitude ionosphere, there are two other potential sources of parallel propagating O^+ in the northern ionosphere. One source is the dayside plasma sheet and another source is the northern high latitude ionosphere. Both of these sources may produce parallel propagating O^+ that is independent of the multiple reconnection sequence illustrated in Figure 1. Although neither of these sources can be conclusively ruled out, there is some evidence that neither contribute significantly to the parallel propagating O^+ observed in the event in Figures 2 through 7. Dayside plasma sheet O^+ typically has a broad energy distribution that includes energies well above 1 keV/e. In contrast, the O^+ flux seen in Figure 2, especially between 1704 and 1714 UT is narrow in energy and peaks below 1 keV/e.

Parallel propagating O^+ that originated in the northern high latitude ionosphere must be produced by coherent reflection or scattering of antiparallel propagating O^+ . Coherent reflection is unlikely because the magnetic field strength decreases with increasing altitude in the cusp. Scattering should produce a broad energy distribution and the distribution in Figure 2 between 1704 and 1714 UT is narrow in energy.

Since neither of these sources for parallel propagating O^+ in the high latitude northern ionosphere can be conclusively ruled out, not all of the 10% of the events that show evidence for parallel propagating O^+ (Table 3) should be considered as evidence of multiple reconnection. As an upper limit of 10%, the frequency of occurrence of closed flux tubes of solar wind ions on the dayside appears to be too small to be considered a viable candidate for the nearly continuous population of the plasma sheet by solar wind ions.

Finally, although closed flux tubes appear to be rare on the dayside, the results of this study do not rule out the possibility that open field lines are closed as they convect from the dayside to the flanks. If reconnected field lines remain open long enough to convect to the flanks

before closing, then parallel propagating O^+ will not be observed in the northern cusp (i.e., between 1000 and 1400 magnetic local time). Rather, the parallel propagating O^+ from the southern hemisphere will be observed on the flanks, outside of the dayside cusp region. This is essentially the interpretation of an event where parallel propagating O^+ was observed at ~ 1700 magnetic local time [Dempsey *et al.*, 1998]. If this process occurs, then there is still the possibility that solar wind ions will be on closed field lines by the time these field lines convect to the tail and become part of the plasma sheet.

Acknowledgments: The TIMAS investigation is the result of many years of hard work by a team of dedicated scientists and engineers. The retired PI for this investigation is E. G. Shelley. Solar wind plasma and IMF observations used in this study were obtained from the CDAWeb. The authors acknowledge the contributions from the PI of the Wind/MFE, R. Lepping, and the PI of the Wind/SWE, K. Ogilvie to this data resource as well as contributions from the PI of the Polar MFI, C. T. Russell. W. K. Peterson thanks D. Baker and the staff at LASP for their hospitality. Research at Lockheed Martin Advanced Technology Center was conducted under NASA contract NAS5-30302.

Table 1 Occurrence Frequency of Parallel and Antiparallel Propagating O^+ spectra.

Spectra	% with anti-parallel propagating O^+	% with parallel propagating O^+	Total number of spectra
683 eV O^+	48%	2%	1278
1.7 keV O^+	34%	4%	1278

Table 2 Occurrence Frequency of Parallel and Antiparallel Propagating O⁺ events.

Events	% with anti-parallel propagating O ⁺	% with parallel propagating O ⁺	Total number of Events
683 eV and/or 1.7 keV O ⁺	80%	10%	60

References

- Berchem, J., J. Raeder, and M. Ashour-Abdalla, Reconnection at the magnetospheric boundary: Results from global magnetohydrodynamic simulations, in *Physics of the Magnetopause*, *Geophys. Monogr. 90*, ed. by P. Song, B. U. Ö Sonnerup, and M. F. Thomsen, p. 205, AGU, Washington, D. C., 1995.
- Crooker, N. Dayside merging and cusp geometry, *J. Geophys. Res.*, *84*, 951, 1979.
- Dempsey, D. L., J. L. Burch, M. M. Huddleston, C. J. Pollock, J. H. Waite, Jr., M. Wüest, T. E. Moore, and E. G. Shelley, Reflected solar wind ions and downward accelerated ionospheric ions during the January 1997 magnetic cloud event, *Geophys. Res. Lett.*, *25*, 2979, 1998.
- Dungey, J. W., The structure of the ionosphere, or adventures in velocity space, in *Geophysics: The Earth's Environment*, edited by C. DeWitt, J. Hiebolt, and A. Lebeau, p. 526-536, Gordon and Breach, New York, 1963.

- Fuselier, S. A., Kinetic aspects of reconnection at the magnetopause, in *Physics of the Magnetopause, Geophys. Monogr. 90*, ed. by P. Song, B. U. Ö Sonnerup, and M. F. Thomsen, p. 181, AGU, Washington, D. C., 1995.
- Fuselier, S. A., B. J. Anderson, and T. G. Onsager, Particle signatures of magnetic topology at the magnetopause: AMPTE/CCE observations, *J. Geophys. Res.*, *100*, 11,805, 1995.
- Fuselier, S. A., B. J. Anderson, and T. G. Onsager, Electron and ion signatures of field line topology at the low-shear magnetopause, *J. Geophys. Res.*, *102*, 4847, 1997.
- Fuselier, S. A., S. M. Petrinec, and K. J. Trattner, Stability of the high-latitude reconnection site for steady northward IMF, *Geophys. Res. Lett.*, *27*, 473, 2000.
- Gosling, J. T., M. F. Thomsen, S. J. Bame, R. C. Elphic, and C. T. Russell, Observations of reconnection of interplanetary and lobe magnetic field lines at the high-latitude magnetopause, *J. Geophys. Res.*, *96*, 14,097, 1991.
- Kessel, R. L., S.-H. Chen, J. L. Green, S. F. Fung, S. A. Boardsen, L. C. Tan, T. E. Eastman, J. D. Craven, and L. A. Frank, Evidence of high-latitude reconnection during northward IMF: Hawkeye observations, *Geophys. Res. Lett.*, *23*, 583, 1996.
- Lennartsson, W., A scenario for solar wind penetration of Earth's magnetic tail based on ion composition data from the ISEE 1 spacecraft, *J. Geophys. Res.*, *97*, 19,221, 1992.
- Lepping, R. P., et al., The wind magnetic field investigation, in *The Global Geospace Mission*, ed. by C. T. Russell, p. 207, Kluwer Academic Publishers, Dordrecht, 1995.
- Maezawa, K. Magnetospheric convection induced by the positive and negative z components of the interplanetary magnetic field: Quantitative analysis using polar cap magnetic records, *J. Geophys. Res.*, *81*, 2289, 1976.

- Newell, P. T., and C.-I. Meng, Mapping the dayside ionosphere to the magnetosphere according to particle precipitation characteristics, *Geophys. Res. Lett.*, *19*, 609, 1992.
- Nishida, A., Can random reconnection on the magnetopause produce the low-latitude boundary layer, *Geophys. Res. Lett.*, *16*, 227, 1989.
- Onsager, T. G., M. F. Thomsen, J. T. Gosling, and S. J. Bame, Electron distributions in the plasma sheet boundary layer: Time-of-flight effects, *Geophys. Res. Lett.*, *17*, 1837, 1990.
- Peterson, W. K., Ion injection and acceleration in the polar cusp, in *The Polar Cusp*, ed. J. A. Holtet and A. Egeland, p. 67, D. Reidel, Dordrecht, 1985.
- Russell, C. T., R. C. Snare, J. D. Means, D. Pierce, D. Dearborn, M. Larson, G. Barr, and G. Le, The GGS/Polar magnetic fields investigation, in *The Global Geospace Mission*, ed. by C. T. Russell, p. 563, Kluwer Academic Publishers, Dordrecht, 1995.
- Russell, C. T., J. A. Fedder, S. P. Slinker, X.-W. Zhou, G. Le, J. G. Luhmann, F. R. Fenrich, M. O. Chandler, T. E. Moore, and S. A. Fuselier, Entry of the POLAR spacecraft into the polar cusp under northward IMF conditions, *Geophys Res. Lett.*, *25*, 3015, 1998.
- Shelley, E. G., et al., The toroidal imaging mass-angle spectrograph (TIMAS) for the Polar mission, in *The Global Geospace Mission*, ed. by C. T. Russell, p. 497, Kluwer Academic Publishers, Dordrecht, 1995.
- Song, P., and C. T. Russell, Model of the formation of the low-latitude boundary layer for strongly northward interplanetary magnetic field, *Geophys Res. Lett.*, *97*, 1411, 1992.
- Sonnerup, B. U. Ö., G. Paschmann, T.-D. Phan, Fluid aspects of reconnection at the magnetopause: In situ observations, in *Physics of the Magnetopause, Geophys. Monogr. 90*, ed. by P. Song, B. U. Ö Sonnerup, and M. F. Thomsen, p. 167, AGU, Washington, D. C., 1995.

Hultqvist, B., M. Øieroset, G. Paschmann, and R. Treumann, Plasma transfer processes at the magnetopause, in *Magnetospheric Plasma Sources and Losses*, Transport across the magnetopause, Kluwer Academic Publishers, Dordrecht, 1999.

Woch J., and R. Lundin, Magnetosheath plasma precipitation in the polar cusp and its control by the interplanetary magnetic field, *J. Geophys. Res.*, *97*, 1421, 1992.

Wu, C. C., Shape of the magnetosphere, *Geophys. Res. Lett.*, *10*, 545, 1983.

Yau, A. W., E. G. Shelley, W. K. Peterson, and L. Lenchyshyn, Energetic auroral and polar ion outflow at DE 1 altitudes: Magnitude, composition, magnetic activity dependence, and long-term variations, *J. Geophys. Res.*, *90*, 8417, 1985.

Figure Captions

Figure 1. Schematic of multiple reconnection on the dayside magnetosphere. Field lines 1 through 4 show the multiple reconnection sequence. Draped magnetic field lines in the magnetosheath (1), reconnect poleward of the southern cusp (2). The reconnected field line convects sunward and the location where the field line crosses the magnetopause moves northward (3). This field line may reconnect again in the northern high latitude region (4). O^+ from the ionosphere propagates along the magnetic field line and is observed as a ~ 1 keV/e field-aligned beam in the subsolar region [Fuselier *et al.*, 1997]. This field-aligned beam has the same propagation direction as the energetic electrons observed on the reconnected field lines that lie sunward of the magnetopause (field lines 2 and 3). If the field line reconnects again in the high latitude northern ionosphere, then a beam of O^+ should be observed propagating parallel to the magnetic field in the northern cusp.

Figure 2. Energy-time spectrogram of a cusp crossing on 11 October 1997. The poleward edge of the cusp is encountered intermittently starting at 1620 UT as indicated by the increase in the H^+ and He^{2+} fluxes above 1 keV/e. Both the H^+ and the He^{2+} exhibit an energy-time dispersion consistent with reconnection at high latitudes. O^+ exhibits the same energy-latitude dispersion. After 1704 UT until the equatorial edge of the cusp at 1712 UT, the O^+ flux increases dramatically.

Figure 3. Polar spacecraft position on 11 October 1997 at 1630 UT. The spacecraft was located on a lobe field line that was reconnecting at a location approximately $4.5 R_E$ above the spacecraft

position. The right hand side shows an H^+ distribution observed near this time period. There are two populations, one propagating parallel to the magnetic field with a velocity of about 300 km/s and the other propagating antiparallel to the magnetic field with a velocity of about 600 km/s. Both populations have cutoff velocities labeled V_e and V_m in the cut through this distribution along the magnetic field.

Figure 4. Mass spectrum of ions parallel (open circles) and antiparallel (solid circles) to the magnetic field at 1.72 keV/e. At this time, there was H^+ and He^{2+} propagating parallel and antiparallel to the magnetic field but the O^+ was propagating only antiparallel to the magnetic field (outflow from the northern ionosphere).

Figure 5. Mass spectra similar to the one in Figure 4 at two different energies during the period in Figure 2 when the O^+ flux increased dramatically. During this time, O^+ is propagating both parallel and antiparallel to the magnetic field.

Figure 6. Countrate (normalized to H^+) for antiparallel propagating 1.72 and 0.68 keV/e O^+ for the cusp interval in Figure 2. After 1645 UT, O^+ is first seen at 1.72 keV/e and then later at 0.68 keV/e. This is the same energy-latitude dispersion that occurs for H^+ and He^{2+} in Figure 2.

Figure 7. Same as Figure 6 for parallel propagating O^+ . Parallel propagating O^+ is observed only near the equatorial edge of the cusp after 1700 UT.

Northward IMF High-Latitude Reconnection

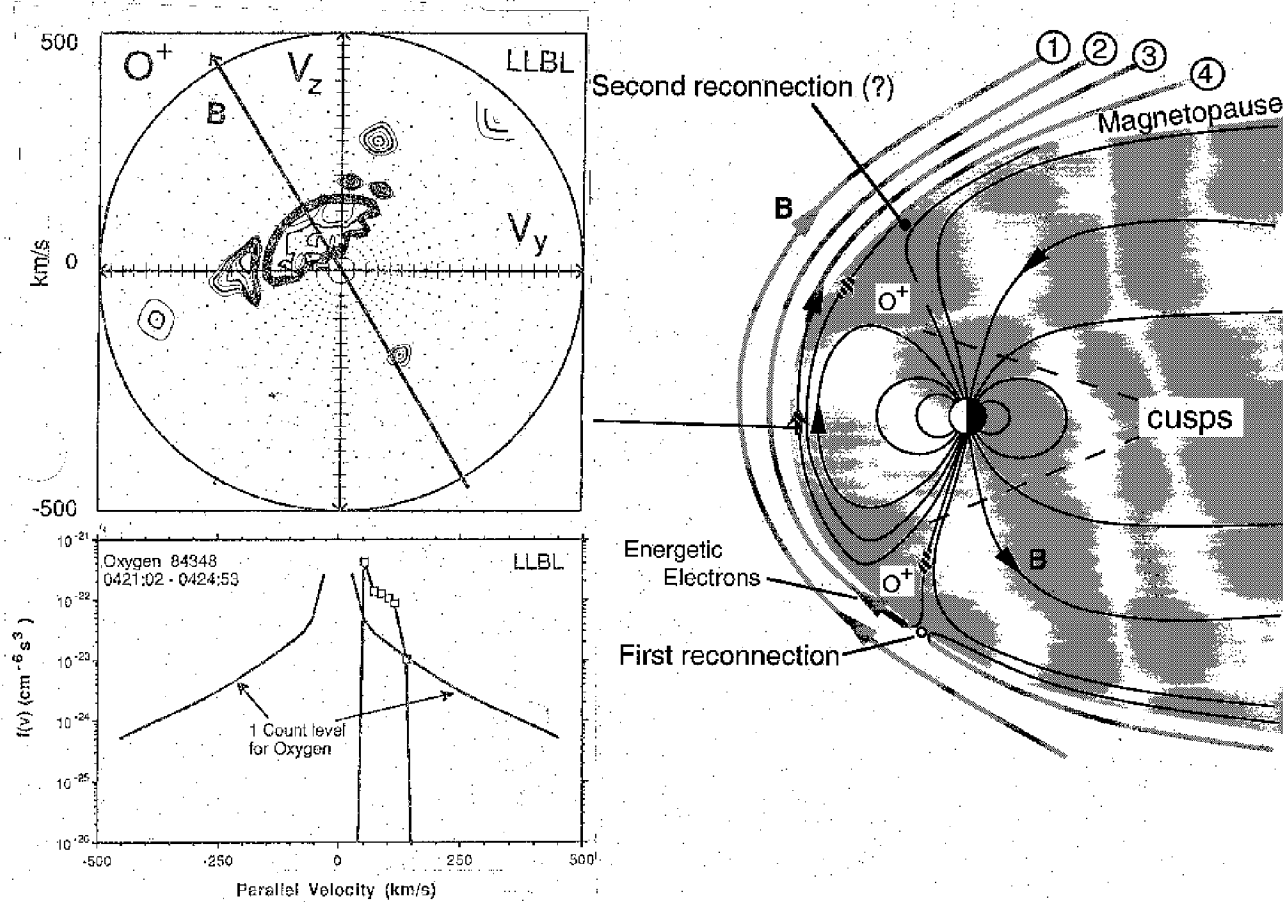
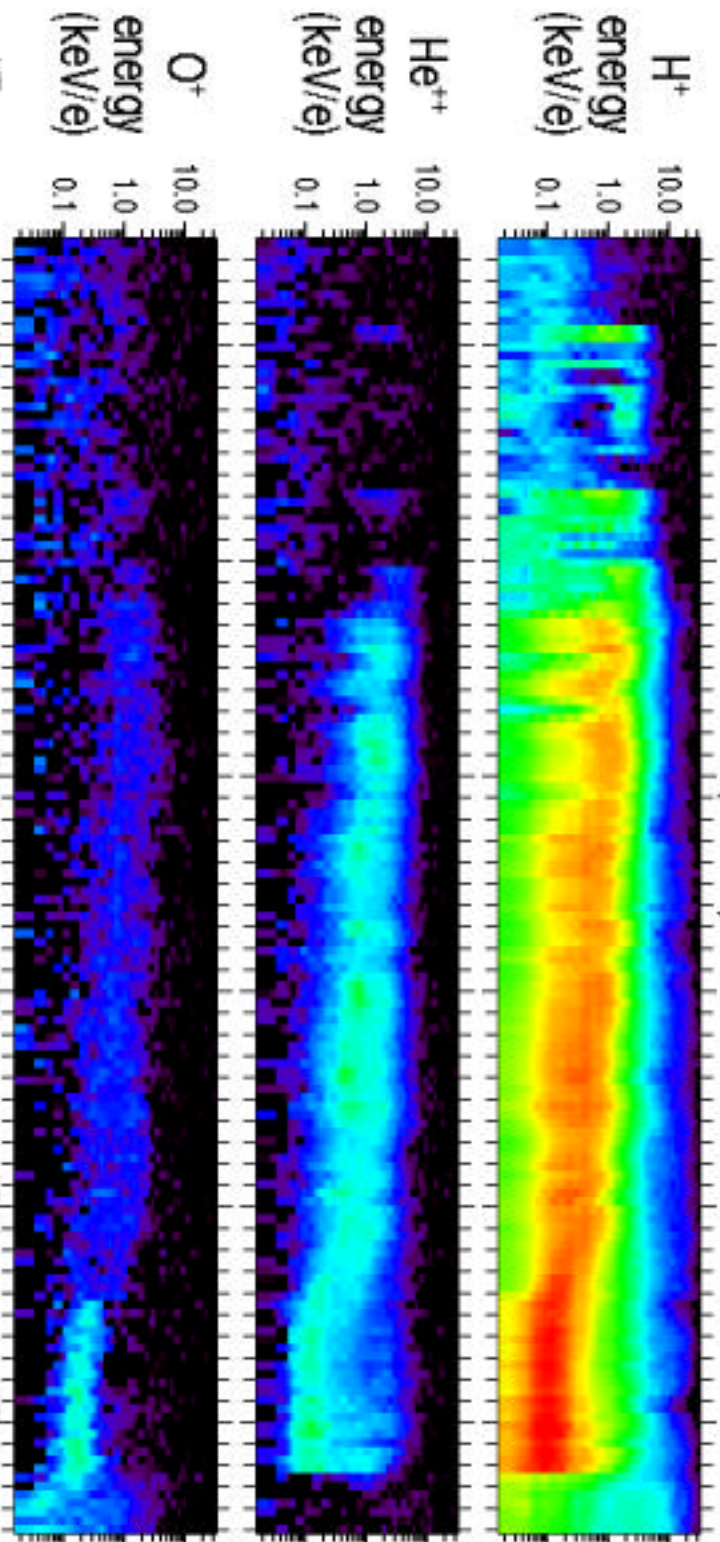


Figure 1

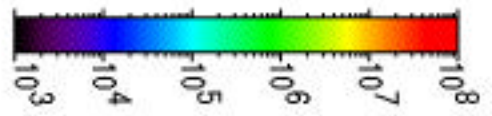
Polar / Timas: 11-OCT-1997 (97284)



UT
R
L
EDMILT
MAGLAT
INVLAT
LT

Averaging period: 4 spins

Wed Apr 12 17:54:35 2000



Flux (1/(cm² sr s keV/e))

Relative Countrate

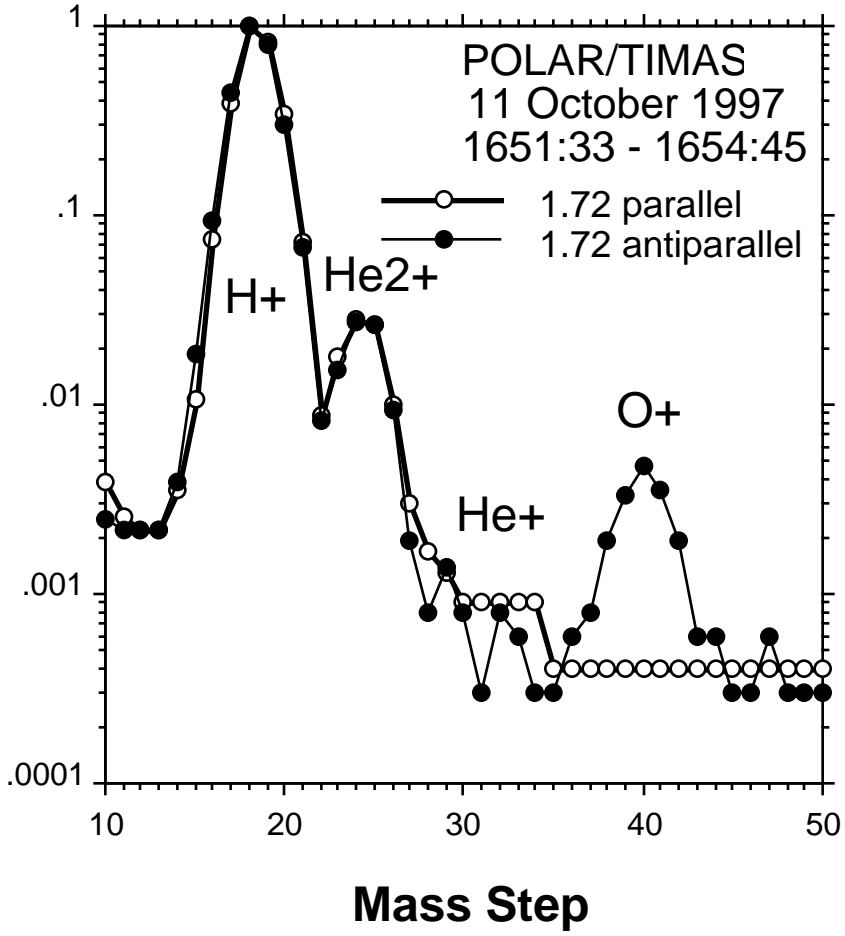
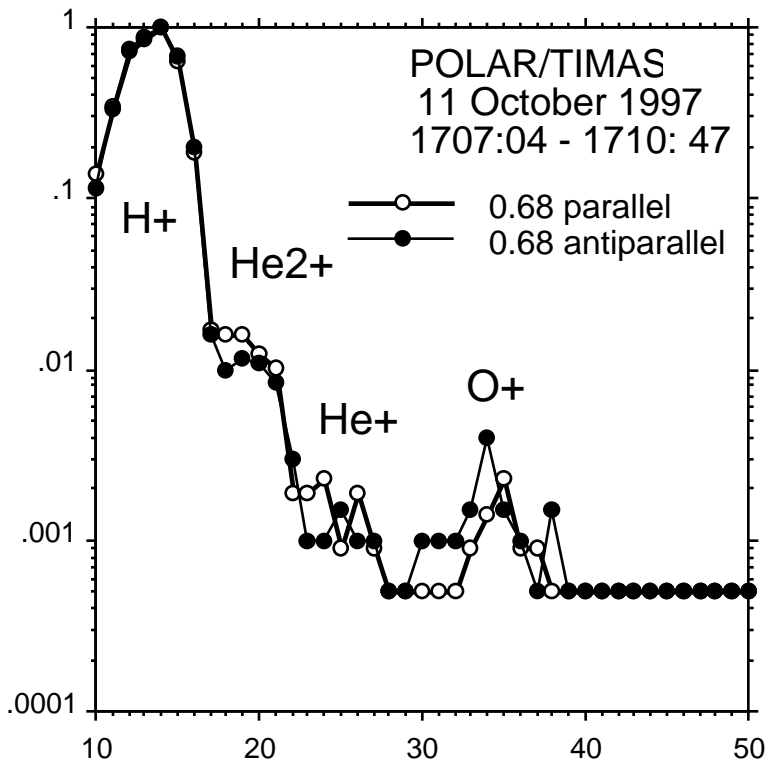
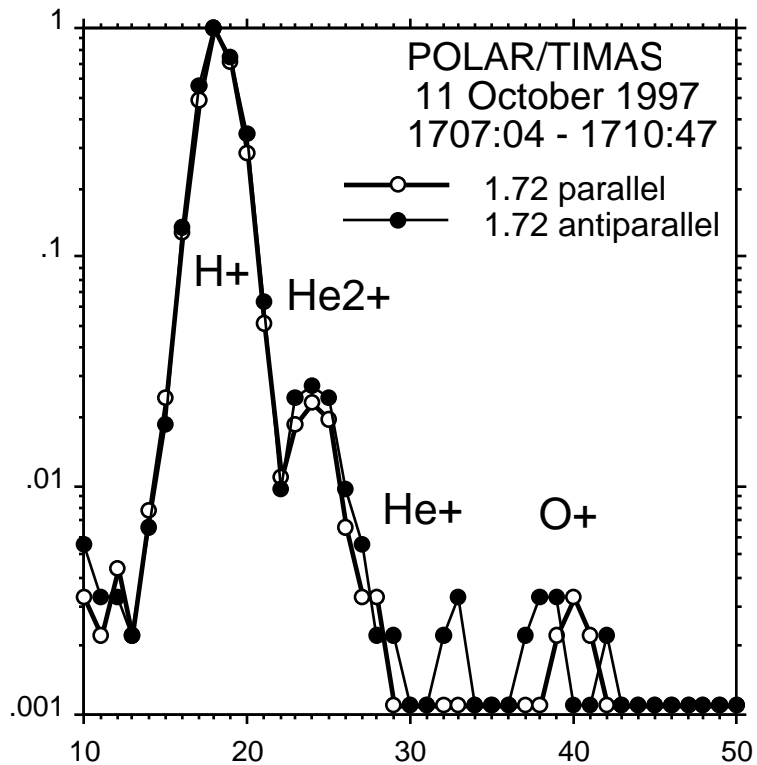


Figure 4

Relative Countrate



Relative Countrate



Mass Step

Figure 5

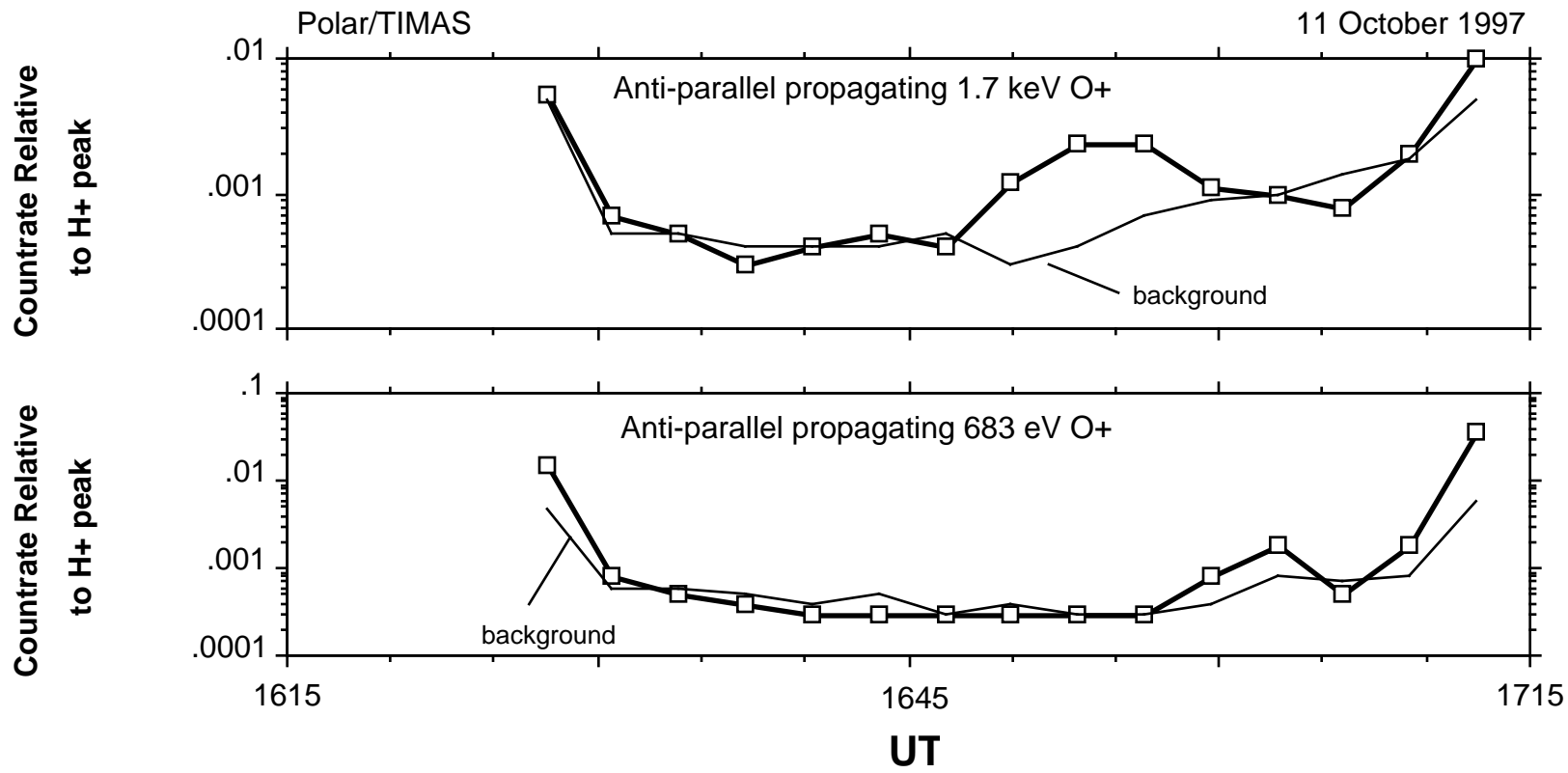


Figure 6

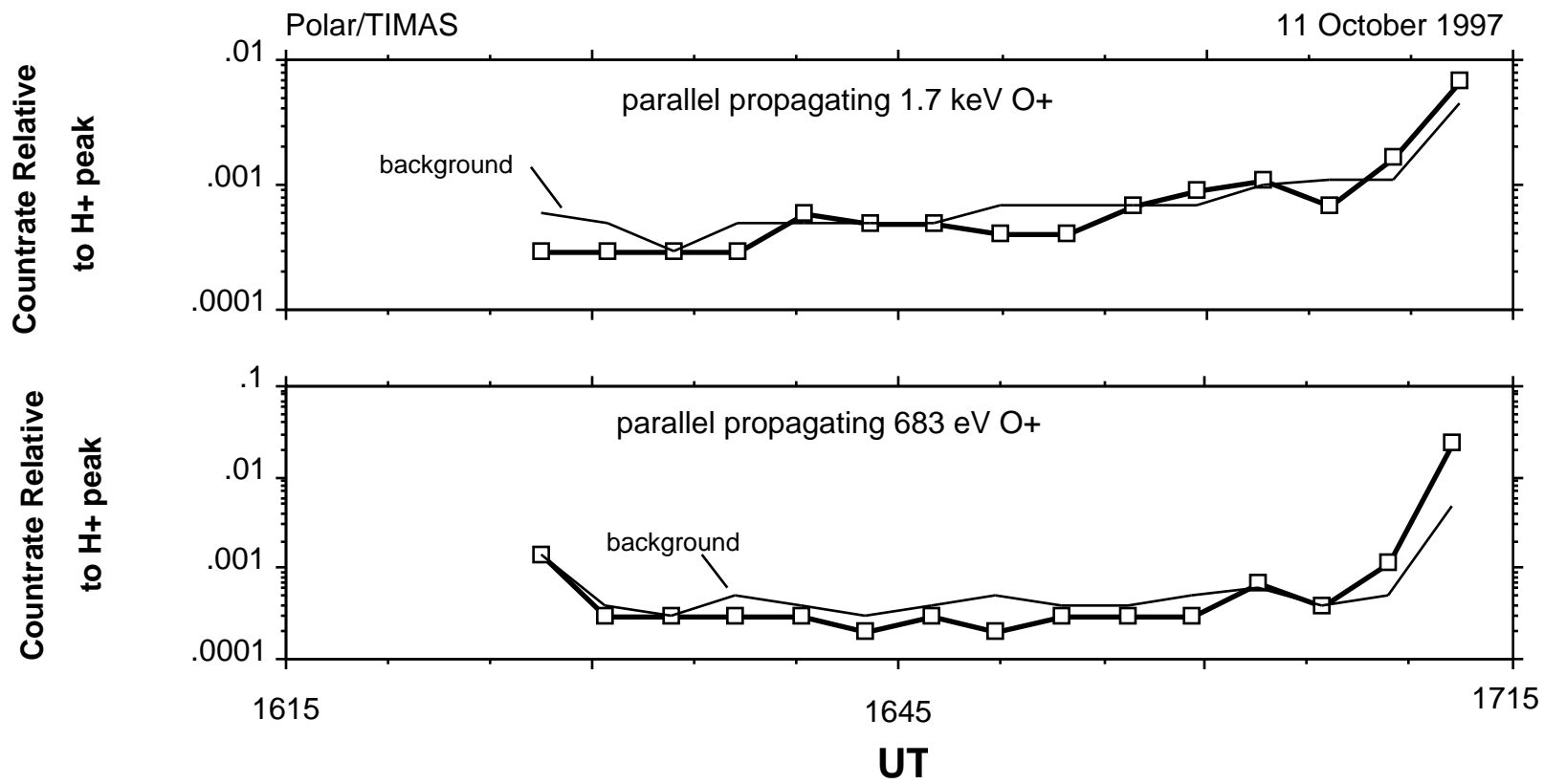


Figure 7